

Results and status of the CRESST experiment

W Rau¹, G Angloher², I Bavykina², M Bauer³, C Bucci⁴, P Christ²,
C Coppi¹, C Cozzini⁵, F von Feilitzsch¹, D Hauff², S Henry⁵,
C Isaila¹, T Jagemann³, J Jochum³, M Kimmerle³, J Koenig¹,
H Kraus⁵, B Majorovits⁵, V Mikhailik⁵, J Ninković², E Pantić²,
F Petricca², W Potzel¹, F Pröbst², Y Ramachers⁶, M Razeti¹,
K Rottler³, S Scholl³, W Seidel², M Stark¹, L Stodolsky²,
A J B Tolhurst⁵, W Westphal¹ and H Wulandari¹

¹ Physik Department E15, Technische Universität München,
James-Franck-Straße, D-85748 Garching, Germany

² Max-Planck-Institut für Physik, Föhringer Ring 6, D-80805 Munich, Germany

³ Physikalisches Institut I, Eberhard Karls Universität Tübingen,
Auf der Morgenstelle 14, D-72076 Tübingen, Germany

⁴ Laboratori Nazionali del Gran Sasso, I-67010 Assergi, Italy

⁵ Department of Physics, University of Oxford, Oxford OX1 3RH, UK

⁶ University of Warwick, Coventry CV4 7AL, UK

E-mail: Wolfgang.Rau @ ph.tum.de

Abstract. CRESST (Cryogenic Rare Event Search with Superconducting Thermometers) employs cryogenic detectors for the direct search for weakly interacting massive dark matter particles (WIMPs). In the second phase of the experiment scintillating calcium tungstate crystals are used to discriminate background by means of different light yield for background and WIMP signals. After first results with this novel technique have been obtained, the experimental setup is being upgraded for further background reduction and larger target mass. The results and present status of the experiment will be presented.

1. Introduction

There is strong observational evidence for the existence of large amounts of non-baryonic dark matter in the universe [1]. However, it is not known up to now what this dark matter might be. Weakly Interacting Massive Particles (WIMPs) are among the best motivated particle candidates to solve this cosmological problem. This hypothesis is supported by the prediction of stable, weakly interacting heavy particles by supersymmetric extensions of the standard model of particle physics [2].

From the rotation curve of our galaxy a local dark matter density of about $0.3 \text{ GeV}/\text{cm}^3$ can be deduced. The assumption of WIMPs being gravitationally bound to the galaxy leads to a characteristic WIMP velocity of around 200 km/s at the position of the Earth. From this the expected energy transfer to ordinary matter can be deduced to be in the order of a few tens of keV for elastic scattering on atomic nuclei.

CRESST (Cryogenic Rare Event Search with Superconducting Thermometers) aims to directly detect WIMPs via their elastic scattering on nuclei in a proper target material. Major challenges for such an experiment are the low energies expected from WIMP interactions, the low

interaction rates, and the background from natural radioactivity or cosmic radiation. Cryogenic detectors were chosen to allow the measurement of the low energies with good resolution [3]. Most of the background is from ionizing radiation, which interacts mainly with the electron system of the target. This allows to efficiently discriminate the background when using a scintillating target since the scintillation efficiency is much lower for nuclear recoils than for electron recoils [4]. For a coherent interaction of WIMPs with a nucleus, the cross section should strongly increase with the atomic mass. Therefore the detector material chosen by CRESST is CaWO_4 , which is a good scintillator also at low temperatures and contains the heavy element tungsten ($A \sim 180$) as a suitable target for WIMP interactions.

2. The CRESST detector modules

The CRESST detectors are based on cylindrical CaWO_4 single crystals with diameter and height of 40 mm and a resulting mass of ~ 300 g. The thermal readout is performed by a superconducting tungsten film in its transition to the normal conducting state (Transition Edge Sensor or TES). The resistance thus strongly depends on the temperature and is measured with a two-armed parallel readout circuit, where the bias current is split between the sensor in the one arm and the input coil of a SQUID and a bias resistor in series in the other arm. The operating temperature is ~ 10 mK. To keep the film at the desired point in its transition, it is equipped with a heater, regulated by an active feedback loop. The stability of the detector response is monitored by means of a set of test pulses injected regularly through the same heater.

To determine the energy of an event, a template pulse is fitted to the measured pulse, where the scaling factor is proportional to the deposited energy. The energy calibration is performed with a set of heater test pulses of known relative energy. The absolute energy scale is determined with the 122 keV and 136 keV lines from a ^{57}Co source. The 46.5 keV line from a ^{210}Pb contamination confirmed the energy scale determined in this way to within about 1 %. The energy resolution is about 1 keV (FWHM) for this line.

Pulses above a few hundred keV saturate the sensor, however the energy can still be determined when only the lower part of the pulse is fitted. This leads to a linear energy scale up to several MeV as has been confirmed by a calibration with a ^{232}Th source, which provides a γ -line of about 2.6 MeV (from ^{208}Th), and also by a set of α -lines from contaminations of the crystal with traces of Uranium and Thorium. The energy resolution of the 2.3 MeV α -line from a ^{147}Sm contamination is 6.7 keV.

An energy threshold of a few keV can be reached. For the most recent low background measurement a hardware threshold of 5 keV has been applied and a 100 % trigger efficiency has been confirmed throughout the measurement period.

The total scintillation light output for CaWO_4 has been determined to be in the range of about 1 % of the total energy deposition for electron recoil events at the given experimental conditions, which requires a very sensitive light detector operating at low temperatures. The detector of choice is a cryogenic detector based on a Silicon substrate ($30 \times 30 \times 0.4 \text{ mm}^3$). The thermal signal induced by the light absorption is again measured with a tungsten TES. Both the CaWO_4 crystal and the light detector are enclosed by a reflective housing to guarantee an efficient light collection. The energy threshold reached with the light detector is of the order of a few tens of eV, corresponding to a few keV energy deposition for an electron recoil event in the CaWO_4 crystal.

A more detailed description can be found in [5]. For the analysis of the high energy part of the spectrum see [6].

3. The experimental setup at Gran Sasso

The experimental setup consists of a $^3\text{He}/^4\text{He}$ dilution refrigerator with a separated large detector volume connected by a cold finger. The detector volume is surrounded by a heavy

copper and lead shielding, including some lead inside the cryostat, to block the direct line of sight between active parts of the refrigerator and the detectors. To avoid electromagnetic interference the setup is placed in a Faraday cage. The cryostat is mounted on a pneumatic suspension system and the detectors inside the cryostat on a spring-held table to reduce susceptibility to mechanical vibrations. The experiment is placed inside the Gran Sasso underground laboratory providing a shielding of about 3600 m w.e. against cosmic radiation. The remaining rate of cosmic muons is about $1.1/\text{m}^2/\text{h}$. The experimental setup is described in more details in [3].

4. Quenching

The reduction of the light signal from nuclear recoils compared to electron recoils is called “quenching”, the reduction factor consequently “quenching factor” (QF). In a Proof-of-Principle experiment [4] the quenching factor for nuclear recoils has been determined to be 7.4 (a more sophisticated re-analysis of the same data [5] changed this value slightly) in the relevant energy range under the assumption of a single event population. However, the quenching might be different for the three different types of nuclei (O, Ca and W) in the target so it is necessary to determine the three corresponding QFs individually for a correct interpretation of the data. The following subsections describe three different approaches for the QF determination: a detailed analysis of a high-statistic neutron calibration with an Am-Be neutron source, a neutron scattering experiment with a monoenergetic pulsed neutron source and an ion-irradiation experiment in a Time-of-Flight mass spectrometer. A fourth subsection describes additional information on the quenching factors that can be deduced from other measurements.

4.1. Am-Be neutron calibration

Figure 1 shows data from a high-statistic calibration with an Am-Be neutron source (in addition a ^{57}Co source was present). The ratio of light signal to thermal signal (light yield, normalized to 1 for electron recoil events of 122 keV) is plotted versus the total energy (measured by the thermal signal). Two clearly separated bands are seen, representing the electron and nuclear recoil events. If the light output for the three different types of nuclei differed by a large amount and the resolution in the light channel were good enough one would expect three distinct bands for the nuclear recoils. This is not observed, however one can look for a structure in the nuclear recoil band.

For kinematical reasons this band is dominated by oxygen recoil events (energy transfer to the heavier nuclei is less efficient). At low energies the contribution from the heavy nuclei becomes important, but here the light signal is very small and the energy resolution in this measurement too poor to resolve a structure. There is however a region at higher energies (280 keV to 340 keV) with a significant contribution from calcium recoils (about 22 %).

If the light yield of the electron recoil band is histogrammed for a given energy bin, the distribution is found to be gaussian. The histogram of the nuclear recoil band from 280 keV to 340 keV shows a clear asymmetry and can be nicely fitted by two gaussian distributions with the same width and a relative weight of 78 % to 22 %. The width of the distributions is constant with the width of the electron recoil band at the corresponding height of the light signal. If the two distributions are attributed to different recoiling nuclei, the deduced quenching factors are 8.2 ± 0.2 and 13.0 ± 1.7 for oxygen and calcium recoils respectively. This measurement and analysis is discussed in more detail in [7].

The measurement has been performed with detectors specifically designed to stand the high count rates in high statistic calibration measurements [8]. This design unfortunately led to a significant reduction of the resolution of the light channel. We are working on an improvement of the light detection for this type of detectors [9] to also access the lower energy region and possibly get information on the tungsten quenching factor from this type of measurement.

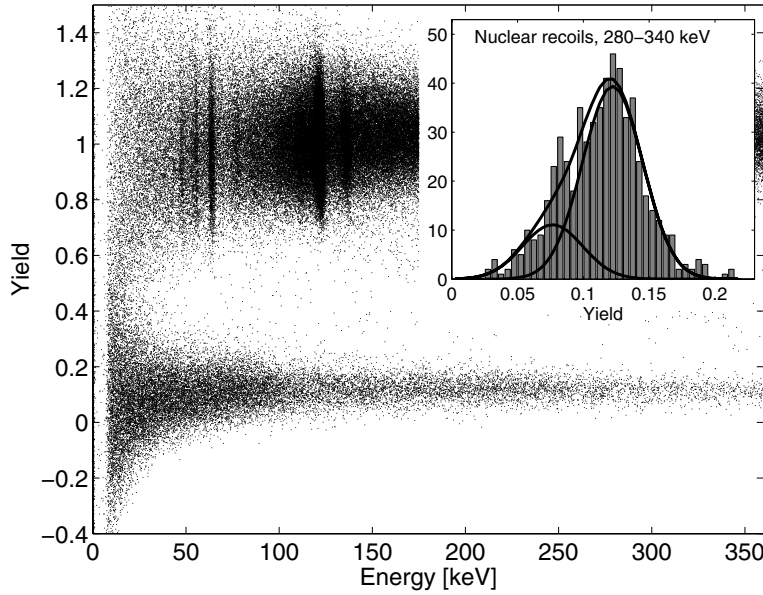


Figure 1. Calibration with an Am-Be neutron source. Shown is the light signal relative to the total energy ('Yield') versus the total energy. The two distinct structures are due to electron recoils (upper band) and nuclear recoils (lower band). The asymmetry of the cross section of the nuclear recoil band at 280-340 keV (inset) is used to deduce the quenching factors for oxygen and calcium in this energy range (see text).

4.2. Neutron scattering experiment

The second method is based on a monoenergetic pulsed neutron source. The energy of the neutrons scattered by the CaWO_4 target under a given angle is measured via their Time-of-Flight (ToF). Thus the kinematics of each event is fully determined and it is possible to deduce the scattering partner. Measuring the light output for the scattering event now allows to calculate the quenching factor.

11-MeV neutrons are produced via the reaction $\text{H}(^{11}\text{Be},n)^{11}\text{C}$ at the tandem Van-de-Graaff accelerator at the Maier-Leibnitz-Laboratory in Garching in bunches with a width of a few ns and a typical bunch spacing of $3.2 \mu\text{s}$ or $6.4 \mu\text{s}$. The scattered neutrons are detected with NE213-scintillation detectors capable of neutron-gamma discrimination via pulse shape. A detailed description of the setup can be found in [10]. A first series of measurements at different scattering angles and recoil energies of 1-2 MeV for oxygen, 0.4-1 MeV for calcium and ~ 100 keV for tungsten has been performed at room temperature, with the light signal being read out by two photomultiplier tubes (PMTs). The quenching factors deduced from this measurement are 12.8 ± 0.5 and 16 ± 4 for oxygen and calcium respectively. For tungsten only a lower limit of 33 (2σ) could be deduced due to the small light signal and some background at low energies [11].

4.3. Ion irradiation

The third method is based on the fact, that the signal at a given energy is expected to be the same for an ion that is produced externally and directed onto the target and for an ion knocked out from its lattice position.

The ions are produced from an external target and accelerated by a potential of 18 kV. Ion source and CaWO_4 crystal are placed in a ToF mass spectrometer, which allows to exactly determine the arrival time of the ion at the target and such an almost background free measurement. The measurements have been performed at room temperature and the light signal is read out by a PMT. This setup is suitable for systematic studies of the behavior of the quenching factor with the atomic mass. A clear trend to higher quenching factors (or lower light output) for larger mass nuclei can be seen. The quenching factors for oxygen, calcium and tungsten determined with this method are 14.1 ± 0.2 , 26.2 ± 0.7 and 40.1 ± 1.3 , respectively [12].

4.4. Additional information on quenching factors

The QF measurements discussed above are performed at different experimental conditions (energy and/or temperature range), which can explain the different numbers obtained for the QFs. Since the conditions are also partially different from the dark matter measurement, we discuss additional experimental results supporting the high QF of 40 for tungsten recoils.

In one high-statistic neutron calibration data set we have observed an additional band corresponding to a quenching factor of 1.5-2, which we attribute to protons from the reaction ($^{40}\text{Ca}(n,p)^{40}\text{K}$) [7].

In our low background data sets we observe a set of lines with a quenching factor of about 5, which can nicely be traced to α -decays from a small contamination of our crystals with uranium and thorium [6].

In one of our low-background data sets we have observed a population of events with a quenching factor of roughly 50, grouped around 100 keV. We attribute these events to a ^{210}Po contamination at the surface of the crystal or the surrounding material. The α -decay of ^{210}Po leads to a recoiling ^{206}Pb nucleus with an energy of 104 keV which may hit the crystal to produce a nuclear recoil event. We confirmed this hypothesis by introducing a scintillation layer in front of the reflector. If the α -particle from the decay hits the scintillation layer, additional light is produced. In this way we could reduce the population of events with QF 50 and observe an additional group of events at the same energy, but with a significant light signal and a different time constant for the scintillation light emission [5].

These three observations concerning the quenching of protons (or hydrogen), α -particles (or helium) and lead clearly confirm the trend to a higher quenching factor for heavier nuclei under the same or very similar experimental conditions as the low background measurements. The mass of the lead and tungsten nuclei are similar enough that, given the quenching factor of 50 for lead, the assumption of a quenching factor of 40 for tungsten, as measured at room temperature, is justified.

5. Dark matter search data

In early 2004 low background data have been collected for about two months with two detector modules and a total exposure of 20.6 kg-days. Electron and nuclear recoils could reasonably well be separated down to 12 keV which was chosen as analysis threshold. Assuming a standard velocity distribution, no WIMP events are expected above 40 keV for a mass range from 10 to 1000 GeV, which sets the upper limit for the analysis region.

Since no neutron moderator or muon veto was present, the sensitivity of the measurement was limited by neutron background. From Monte Carlo simulations we expect a neutron rate of about 0.6 events/kg/day in the energy range from 12 keV to 40 keV from radioactivity in the surrounding rock and concrete and about a factor of three less from muon interaction in the lead shielding [13].

The observed number of events in the analysis region, limited in light yield by a 90 % upper limit for oxygen recoil events, was 16. Taking into account the exposure and the acceptance of 90 %, this translates into a rate of (0.87 ± 0.22) events/kg/day.

One of the two detector modules showed an energy resolution good enough that tungsten recoil events with QF of 40 could be separated from the oxygen recoil region. In this module with an exposure of 10.7 kg-days there was no event in the 90 % acceptance region for these tungsten events in the energy range of interest.

For a conservative analysis we have considered the whole nuclear recoil region, with no assumption on the origin of the events. We also analyzed the data from the module with the better energy resolution alone under the assumption of a QF of 40 for tungsten recoils. Figure 2 shows the two 90 % upper limits for the WIMP-nucleon cross section for spin-independent interaction calculated using the “optimal interval” method [14], under the standard assumptions

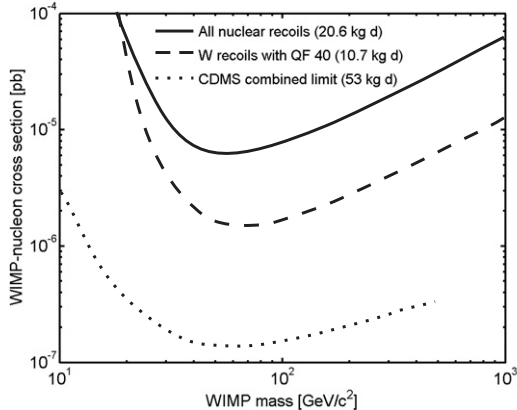


Figure 2. Upper limits on the spin-independent WIMP-nucleon interaction cross section (standard halo properties assumed, see text). The upper (solid) line conservatively takes all nuclear recoil events into account, while the lower (dashed) line is deduced only from the region expected for tungsten recoil events with a QF of 40 in the detector with the better resolution (see text). For a comparison the presently most stringent experimental limit, achieved by CDMS [17], is shown (dotted curve).

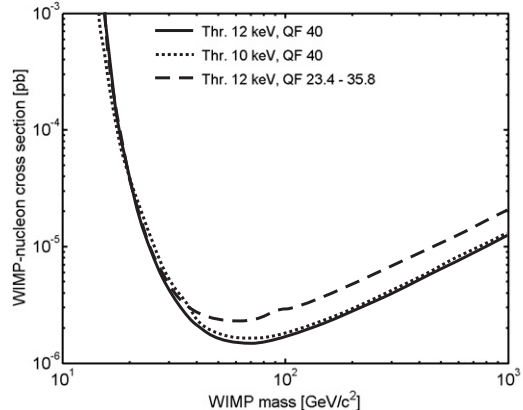


Figure 3. The more stringent limit from Figure 2 is compared to the limits deduced when the threshold is lowered to 10 keV (2 events at 10.5 and 11.3 keV) or when a lower QF for tungsten recoils ($23.4 < \text{QF} < 35.8$) is assumed (one event at 22.2 keV).

on the WIMP halo (isothermal halo, WIMP characteristic velocity: 220 km/s, mean Earth velocity: 232 km/s, local WIMP density: $0.3 \text{ GeV}/c^2/\text{cm}^3$) and the WIMP interaction (we used the Helm spin-independent form factor for the nucleus [15] with the parameterization from [16] and A^2 scaling for coherence). For a comparison, the best present limit, achieved by CDMS [17], is also shown. The complete analysis is described in [5].

We have also tested the robustness of the more stringent limit against variations of threshold and QF. If we change the analysis threshold from 12 keV to 10 keV, 2 events fall into the analysis region. The resulting limit, however, is almost unchanged (see Figure 3). If the QF is varied, one event at 22.2 keV enters the analysis region for a QF of less than 35.8. In this case the limit moves up by about 50 % (from 1.6 to 2.3×10^{-6} pb for 60 GeV WIMPs, see Figure 3). This limit is unchanged (no additional event) if QFs down to 23.4 are assumed. About the same change for the limit is observed, when, in disregard of the worse resolution, also the data from the second detector are included in the analysis with the high quenching factor (QF of 40, threshold 12 keV; in this case the exposure is again 20.6 kg-days and 3 events are in the analysis region). This investigation demonstrates the robustness of our analysis against changes of those analysis criteria, which possibly have an unknown contribution to the systematic uncertainty.

6. Upgrade of the setup

Since April 2004 the experimental setup is being upgraded. A muon veto detector consisting of 20 plastic scintillator panels and a 50 cm polyethylene shielding have been installed to reduce the neutron background. To allow an increase of the detector mass up to 10 kg or 33 detector modules, a new 66 channel SQUID system has been installed. The detector integration system for the 33 detector modules is being produced. Also most parts of the new readout electronic and

data acquisition system are ready or being prepared. A restart of the measurement is planned for early 2006, increasing the detector mass step by step to 10 kg.

7. Conclusions

CRESST demonstrated the potential of the combination of cryogenic detectors with the detection of scintillation light for very efficient background discrimination. First low background data have been taken and a sensitivity for the elastic scattering cross section for spin-independent interaction between WIMPs and nucleons of about 1.6×10^{-6} pb for WIMP masses around 60 GeV has been reached. The sensitivity was limited by background neutrons produced from natural radioactivity in the surrounding rock and cosmic ray muons in the lead shielding.

Presently the experimental setup is being upgraded by a neutron moderator and a muon veto detector for a reduction of the neutron background, and by a new 66 channel SQUID system which will allow to increase the total detector mass up to 10 kg. After the restart, planned in early 2006, the sensitivity shall be increased step by step by about two orders of magnitude.

Acknowledgments

This work has been supported in part by the DFG via SFB 375; the EU via the networks for Cryogenic Detectors (ERB-FMRXCT980167) and for Applied Cryogenic Detectors (HPRN-CT2002-00322), via ILIAS (RII-CT-2004-506222) and the Marie Curie Fellowship program; the HGF via the virtual institute VIDMAN (VH-VI-033); the DAAD; PPARC; the INFN and the MLL, Garching. We would like to thank the INP Lyon for providing part of the hardware for the neutron scattering experiment.

References

- [1] Bergström L 2000 *Rep. Prog. Phys.* **63** 793-841
- [2] see e.g. Jungman G, Kamionkowski M and Griest K 1996 *Phys. Rep.* **267** 195-373
- [3] Angloher G *et al* 2002 *Astropart. Phys.* **18** 43-55
- [4] Meunier P *et al* 1999 *Appl. Phys. Lett.* **75** 1335-7
- [5] Angloher G *et al* 2005 *Astropart. Phys.* **23** 325-39
- [6] Cozzini C *et al* 2004 *Phys. Rev. C* **70** 064606
- [7] Stark M 2005 Detektoren mit effizienter und schneller Phononensammlung für das CRESST-Experiment *PhD thesis Technische Universität München* available via <http://mediatum.ub.tum.de/mediatum/>
- [8] Stark M *et al* 2004 *Nucl. Instrum. Methods A* **520** 197-200
- [9] Stark M, Boslau O, Feilitzsch F von, Goldstraß P, Jochum J, Kemmer J, Potzel W and Rau W 2005 *Nucl. Instrum. Methods A* **545** 738-43
- [10] Jagemann T, Feilitzsch F von and Jochum J 2005 *Nucl. Instrum. Methods A* **551** 245-60
- [11] Jagemann T 2004 Measurement of the Scintillation Light Quenching for Nuclear Recoils induced by Neutron Scattering in Detectors for Dark Matter Particles *PhD thesis Technische Universität München* available via <http://mediatum.ub.tum.de/mediatum/>
- [12] Ninković J *et al* 2005 New Technique for the Measurement of the Scintillation Efficiency of Nuclear Recoils submitted to *Nucl. Instrum. Methods A* (*Preprint* <http://publications.mppmu.mpg.de/2005/MPP-2005-133/FullText.pdf>)
- [13] Wulandari H *et al* 2003 Neutron Background Studies for the Dark Matter Experiment CRESST *Preprint* hep-ex/0401032
- [14] Yellin S 2002 *Phys. Rev. D* **66** 32005.
- [15] Helm R H 1956 *Phys. Rev.* **104** 1466-75
- [16] Lewin J D and Smith P F 1996 *Astropart. Phys.* **6** 87-112
- [17] Akerib D S *et al* 2005 Limits on spin-independent WIMP-nucleon interactions from the two-tower run of the Cryogenic Dark Matter Search *Preprint* astro-ph/0509259